JACS
JOURNAL OF THE AMERICAN CHEMICAL SOCIETY

COMMUNICATION

pubs.acs.org/JACS

Crystallographic X-ray Analyses of Yb@C_{2v}(3)-C_{80} Reveal a Feasible Rule That Governs the Location of a Rare Earth Metal inside a Medium-Sized Fullerene

Xing Lu,[†] Yongfu Lian,[‡] Christine M. Beavers,[§] Naomi Mizorogi,[†] Zdenek Slanina,[†] Shigeru Nagase,[*,∥] and Takeshi Akasaka[*,†]

[†]Center for Tsukuba Advanced Research Alliance, University of Tsukuba, Tsukuba, Ibaraki 305-8577, Japan

[‡]School of Chemistry and Materials Science, Heilongjiang University, Harbin 305-0801, China

[§]Advanced Light Source, Lawrence Berkeley National Laboratory, Berkeley, California 94720, United States

[∥]Department of Theoretical and Computational Molecular Science, Institute for Molecular Science, Okazaki, Aichi 444-8585, Japan

Supporting Information

ABSTRACT: Single crystal X-ray diffraction studies of Yb@C_{2v}(3)-C_{80}·Ni^{II}(OEP)·CS_2·1.5C_6H_6 (OEP = octaethylporphinate) reveal that a relatively flat region of the fullerene interacts with the Ni^{II}(OEP) molecule, featuring shape-matching interactions. Surprisingly, it is found that the internal metal is located under a hexagonal carbon ring apart from the 2-fold axis of the C_{2v}(3)-C_{80} cage, presenting the first example of metallofullerenes with an asymmetrically positioned metal. Such an anomalous location of Yb^{2+} is associated with its strong ability to pursue a large coordination number and the lack of hexagon along the C_2 axis of C_{2v}(3)-C_{80}. It is accordingly assumed that a suitable cage hexagon is most likely to be preferred by the single rare earth metal to stay behind inside a medium-sized fullerene, such as C_{80} and C_{82}.

Endohedral metallofullerenes (EMFs) are hybrid molecules with metal atoms or metallic clusters encapsulated inside the interior of fullerenes. Intramolecular charge transfer from metal to cage takes place, which is regarded as the main origin of the fascinating properties of EMFs.[1]

Structural determinations of EMFs have played a central role in understanding the metal−cage interactions and their intrinsic properties. The endohedral nature of EMFs was first determined for Y@C_{82} using the synchrotron radiation powder X-ray diffraction coupled with Rietveld treatment and maximum entropy analysis.[2] However, the reliability of this method is rather poor: structures of several EMFs have been wrongly assigned.[3] During recent years, NMR spectrometry, normally with the assistance of theoretical calculations, has shown great success in determining the cage structures of fullerenes and EMFs, even of some paramagnetic species.[4] However, this method could not provide adequate information about the location of the internal metallic species.

Undoubtedly, single crystal X-ray diffraction (XRD) is the most reliable solution for EMF structures, especially in view of the position and motion of the endohedral metals. However, the spherical molecules rotate rapidly within the crystal lattice even though good crystals are obtained, thus, impeding explicit structural determination. To solve this problem, two strategies, exohedral modification[5] and cocrystallization with metal porphyrins,[6] have been developed, and many successful results have been published recently. It is worth noting that exohedral modification inevitably distorts the fullerene cage and thus possibly alters the metal position inside; therefore, the X-ray structures of EMF-derivatives are always different from the true situation of pristine EMFs, though in some cases the difference is very small.[5] Cocrystals of EMFs with metal porphyrins, however, are better suited to illustrate the pristine environment with respect to both cage structures and metal positions if a good single crystal and appropriate crystallographic parameters can be obtained.[6]

Since the first report of the single crystallographic X-ray structure of Sc_3N@C_{80},[7] many EMFs cocrystallized with metal porphyrins have been structurally determined.[6,8] A detailed examination of published results reveals that most of these studies have focused on cluster EMFs and di-EMFs,[6,8] but little is known about the structures of mono-EMFs which actually are the simplest prototypes and ideal candidates for elucidating metal−cage interactions. Ba@C_{74} is the first example of mono-EMFs whose structure has been elucidated using XRD.[9] Because severe disorder exists, theoretical calculations were conducted to help with the assignment of the metal position. The final results showed that the metal is situated at one pole of the molecule along one of the three C_3 axes. Recently, the molecular structures of M@C_{3v}(134)-C_{94} (M = Ca or Tm) were also reported. It is interesting to find that Ca^{2+} is located closely to a [6,6]-junction, while Tm^{2+} prefers to sit under a hexagonal ring, both of which are near the C_3-axis, showing that rare earth metals and alkaline-earth metals prefer different positions inside a same fullerene cage.[10] In addition, the X-ray crystallographic results of the four isomers of Sm@C_{90} indicated that the Sm^{2+} moves rapidly along a cage belt comprised of continuous hexagonal carbon rings.[11] Accordingly, it seems that the dynamic motion of the internal metal is not associated with the cage size but is more likely to be dependent on the metal and the cage structures. Moreover, because the above investigations have focused on either a small cage (C_{74}) or relatively large cages (C_{90} or C_{94}), it is very necessary to investigate the molecular structures with different

Received: May 20, 2011
Published: June 17, 2011

dx.doi.org/10.1021/ja204653z | J. Am. Chem. Soc. 2011, 133, 10772–10775

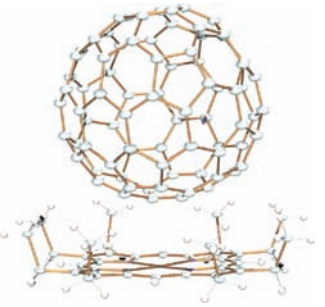

Figure 1. Ortep drawing of Yb@C_{2v}(3)-C_{80}·Ni(OEP) showing ellipsoids at the 50% probability level. Only the major orientation is shown and solvent molecules are omitted for clarity.

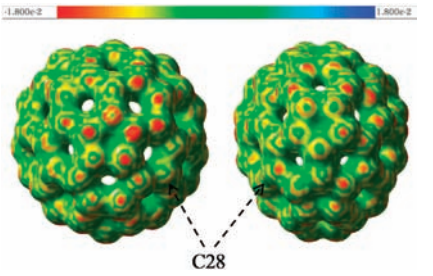

Figure 2. Electrostatic potential mapping on the isosurface of Yb@C_{2v}-(3)-C_{80} as viewed from two orthogonal directions.

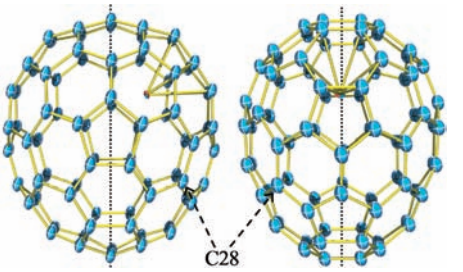

Figure 3. Perspective views of Yb@C_{2v}(3)-C_{80} showing the location of Yb. (Left panel) side view; (right panel) front view. The bonds between Yb and the adjacent hexagonal ring are shown; C28 which is nearest to the pairing Ni^{II}(OEP) is marked to enhance comprehension. The C_2 axis is indicated with a dotted line.

metal contents and other cage sizes comparable to these of abundantly produced $M_3N@C_{80}$ and $M@C_{82}$.

Herein, we report unambiguous X-ray results of Yb@C_{2v}(3)-C_{80}, a medium-sized EMF with a divalent rare earth metal. Yb-EMFs have the lowest production yield and are the last isolated species among all mono-EMFs.[12] Single crystals of Yb@C_{2v}(3)-C_{80}·Ni^{II}(OEP)·CS_2·1.5C_6H_6 were prepared using an interfacial diffusion method in a glass tube (φ7mm). After 10 days, black crystalline rods appeared at the bottom of the tube (Figure S1). A piece of crystal cut from one of these rods was found suitable for XRD determination and provides the structural information of the molecules.

Figure 1 depicts the structure of the endohedral molecule and its relationship to the nickel porphyrin determined at 90(2) K. It is unambiguous that Yb@C_{80} takes the C_{2v}(3)-C_{80} cage which corroborates our previous NMR results.[4a] However, it should be pointed out that this cage is only found for mono-EMFs, such as Yb@C_{80} and La@C_{80}. The latter is not soluble in common solvents and was obtained as its dichlorophenyl derivatives.[13] Other metallic clusters would template different C_{80} cages because of the different number of transferred electrons. For example, the Sc_3N (or La_2) and Sc_2C_2 clusters prefer I_h(7)-C_{80} and C_{2v}(5)-C_{80}, respectively.[14]

It is evident from the crystallographic data that the fullerene and Ni^{II}(OEP) form a 1:1 complex; the vacancy of the crystal cell is occupied by one CS_2 and 1.5 benzene. Although there is disorder of the fullerene structure, the major orientation is particularly well determined. Two orientations of the cage with respective occupancies of 0.634(8) and 0.366(8) are identified, as well as two Yb positions having the same ratio. Accordingly, it is likely that each Yb^{2+} position corresponds to one cage orientation. For clarity, only the major pair is shown in Figure 1. It is worth noting that no structural restraints are applied to the major orientation during the refinement process. Thus, cage structure and metal position are well-defined. A relatively flat region of the C_{2v}(3)-C_{80} cage, where no pentagon is involved, approaches closely to the NiN_4 plane of Ni^{II}(OEP). The shortest nickel−cage carbon distance (Ni1−C28) is 2.818(5) Å, which is similar to the corresponding values reported before, indicating noncovalent interactions between them.[6]

We calculated the electrostatic potentials of Yb@C_{80} based on the X-ray result to further understand the origin of the interactions between the endohedral and Ni^{II}(OEP). Because of the two-electron transfer from Yb to the cage, the surface of C_{80}^{2-} is mostly covered by negative charges. Detailed analysis reveals that C28, as well as its neighboring atoms, is slightly negatively charged (Figure 2), which is contrary to the previous reports concluding that Ni^{II}(OEP) tends to interact with a positively charged cage carbon of D_{5h}(1)-C_{90} and Sm@C_{90} isomers.[11,15] Normally, two factors are responsible for the interactions between fullerenes and Ni^{II}(OEP): shape matching and electrostatic attraction. Since the all-*cis* conformation of the eight ethyl groups in Ni(OEP) results in a highly flat plane consisting of Ni, four N atoms, and the adjacent carbon atoms, it always demands a flat region of the fullerene to approach it. Actually, in the cases of C_{90} and other EMFs, the interaction sites are generally the flattest parts of the cages (no pentagon). Thus, it is inferred that both shape matching and electrostatic interaction are effective factors in dictating the interactions between fullerenes/EMFs and metal porphyrins.

A surprising and unprecedented finding is the anomalous location of the Yb^{2+} cation inside the C_{2v}(3)-C_{80} cage. As clearly shown in Figure 3, the Yb^{2+} is not situated along the 2-fold axis but it asymmetrically coordinates with a hexagonal ring apart from the symmetric axis. The nearest Yb−C distances vary in a narrow range from 2.476(14) to 2.644(12) Å, which are slightly shorter than the normal coordination bond lengths in "π-bonded" complexes of Yb.[16] Short metal−cage distances have been frequently found for $M_3N@C_{2n}$ (M = Sc, Y, Tb, etc.; $2n$ = 68, 78, 80, etc.) where the relatively crowded M_3N should be responsible for such strong metal−cage interactions.[6] However, since only one metal is encapsulated in Yb@C_{80}, the short Yb−cage distances may originate from the strong ability of Yb^{2+} to coordinate with the cage carbons so as to satisfy its valent orbital as much as possible.

The unusual location of Yb^{2+} is obviously different from the metal positions in mono-EMFs found previously using single crystal X-ray crystallography. As mentioned above, the single metal always tends to reside along the symmetric axis either in Ba@C_{74} or in M@C_{94} (M = Ca, Tm). Moreover, though no

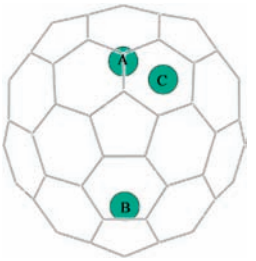

Figure 4. Theoretical considerations of metal position in Yb@C_{2v}(3)-C_{80}. Positions A and B are normal on-axis conformations frequently observed in mono-EMFs, such as M@C_{2v}(9)-C_{82}, while position C is the off-axis conformation corresponding to the current XRD study.

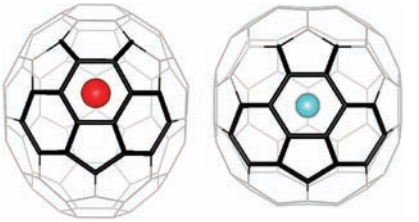

Figure 5. Comparison of the metal environments in Yb@C_{2v}(3)-C_{80} (left) and Y@C_{2v}(9)-C_{82} (right). Both are theoretically optimized structures derived from XRD results.

crystallographic results of pristine M@C_{2v}(9)-C_{82} (M = Sc, Y, La, Ce, Gd, etc.) have been reported, X-ray data of their derivatives and other experimental/theoretical results show that the single metal always tends to stay under a hexagonal ring along the C_2 axis.[5,17] The situation that the single metal tends to stay along one of the symmetric axes is probably because such areas are generally more curved than other parts of the fullerene cage, and accordingly are more suitable for accommodating the metal atom. Moreover, it is well-known that rare earth metals tend to pursue a high coordination number ranging from 6 to even 14. These can be used to explain the fact that the metal in M@C_{2v}-(9)-C_{82} (M = Sc, Y, La, Ce, Gd, etc.) always coordinates with a hexagonal ring, instead of the opposite [6,6]-bond.[4,5]

However, the C_{2v}(3)-C_{80} cage contains no hexagonal ring along the C_2 axis, but only two [6,6]-bonds (cf. Figure 3). Thus, if the Yb^{2+} prefers to stay along the axis, two off-center positions are most probable: A and B (Figure 4). In either case, the Yb^{2+} has to sit on a [6,6]-bond. Position C is the true place of Yb^{2+} found by XRD. We performed theoretical calculations to further understand the abnormal metal position. All calculations were carried out using the Gaussian 03 program package.[18] The molecular structures were first optimized at the B3LYP/3-21G∼CEP level (3-21G basis set[19] for C atoms and CEP-4G basis[20] with the CEP effective core potential (ECP) for Yb) and then reoptimized with the B3LYP/6-31G*∼SDD approach (6-31G* basis[21] for C and SDD basis[22] with the SDD ECP for Yb) both with the B3LYP density functional.[23] Our results reveal that no energy minimum could be found for position A, while even though the Yb^{2+} can stay at position B, this conformation is 6.19 kcal/mol higher in energy than the one with Yb^{2+} located at position C. As a result, it can be concluded that the anomalous endohedral structure of Yb@C_{80} could be a dual effect of both cage geometry and the metal coordination ability. This is an evident example showing that the ability of rare earth metals to pursue a high coordination number may dominate the metal position inside a fullerene cage. It should also be noted that our previous crystallographic work of La@C_{80}($C_6H_3Cl_2$) shows that the La position is nearly identical to that of Yb found in this work, although the cage is somewhat distorted by the covalent linkage of the addend.[13] All the above results lead to the conclusion that a rare earth metal prefers to locate under a suitable hexagonal ring inside a medium-sized fullerene cage, like C_{80} and C_{82}.

The preferred location of the single metal under a hexagonal ring in both M@C_{2v}(3)-C_{80} (M = La, Yb) and M@C_{2v}(9)-C_{82} (M = Sc, Y, La, Ce, Gd, etc.) stimulates us to investigate the metal environments in both cases. Figure 5 shows the optimized structures of Yb@C_{2v}(3)-C_{80} and Y@C_{2v}(9)-C_{82}. It is clear that, although the shape of the two cages differs significantly, the arrangement of the parts closest to the internal metal is mutually similar, both consisting of a central hexagon and adjacent frameworks, as emphasized with black sticks. Thus, it is inferred that such a structure is suitable for accommodation of the single rare earth metal.

Since Yb^{2+} is positioned away from the C_2 axis of C_{2v}(3)-C_{80}, the molecular symmetry is thus reduced from C_{2v} to C_s. Recently, we observed that the internal Sc_2C_2 cluster in Sc_2C_2@C_{2v}(5)-C_{80} has an obvious influence on the molecular symmetry: the strong metal−cage interaction reduces the overall symmetry of the molecule from C_{2v} to C_s at a temperature lower than 353 K.[14] If the metal−cage interaction in Yb@C_{2v}(3)-C_{80} is still so strong at ambient conditions, the molecule should show C_s symmetry, instead of C_{2v}. However, the ^{13}C NMR spectrum obtained at room temperature displays a [17 × 4C, 6 × 2C] pattern, which unambiguously corresponds to C_{2v} symmetry, not C_s (Figure S2).[4a] Thus, it infers that the Yb−cage bonding is loosened at higher temperatures. To confirm this, we performed the XRD measurements at different temperatures. The results show that the metal position is nearly unchanged below 173 K. However, when the temperature is increased to 223 K, one additional metal position is distinguished at an opposite side of the cage, indicating a jumping metal within the cage (Supporting CIF files and Tables S1−S4). Unfortunately, the crystal was decomposed during our room-temperature XRD measurement. Nevertheless, it is still conclusive from the NMR result that the internal metal has no obvious influence on the molecular symmetry: it may be rotating or jumping at room temperature.

In conclusion, we have successfully obtained cocrystals of Yb@C_{2v}(3)-C_{80} and Ni^{II}(OEP) in which both parts are highly ordered, thus, enabling precise structural determination of both the molecular structure of and the metal position in this endohedral. A relatively flat surface of the fullerene cage approaches the plane of the metal porphyrin, featuring shape-matching interactions. More interestingly, the results show that the Yb^{2+} is not situated along the 2-fold axis which ends with two [6,6]-bonds, but it is asymmetrically positioned under a hexagonal ring apart from the axis. In combination with calculations, we attribute such an unusual location of Yb^{2+} to its ability of pursuing a maximum coordinating environment and the lack of hexagon along the C_2 axis of the C_{2v}(3)-C_{80} cage. Thus, it seems that there exists a possible rule that the rare earth metal inside a medium-sized fullerene cage (e.g., C_{80} and C_{82}) prefers to reside under a hexagonal ring, instead of sitting above a C−C bond. Our results have provided fundamentally new insights into the structure of pristine EMFs and metal−cage interactions, which will be useful to predict the metal positions in mono-EMFs in future works. It is also expected that such an

anomalous metal position will have a strong influence on the chemical behaviors of cage carbons.

■ ASSOCIATED CONTENT

Supporting Information. Complete refs 3b, 4b, 5b, and 18, experimental details, photograph of single crystals and X-ray data. This material is available free of charge via the Internet at http://pubs.acs.org.

■ AUTHOR INFORMATION

Corresponding Author
akasaka@tara.tsukuba.ac.jp; nagase@ims.ac.jp

■ ACKNOWLEDGMENT

This work is supported in part by a Grant-in-Aid for Scientific Research on Innovative Areas (No. 20108001, "pi-Space"), a Grant-in-Aid for Scientific Research (A) (No. 20245006), The Next Generation Super Computing Project (Nanoscience Project), Nanotechnology Support Project, Grants-in-Aid for Scientific Research on Priority Area (Nos. 20036008, 20038007), and Specially Promoted Research (No. 22000009) from the Ministry of Education, Culture, Sports, Science, and Technology of Japan, and The Strategic Japanese-Spanish Cooperative Program funded by JST and MICINN. Y.L. thanks the financial support from the National Natural Science Foundation of China (No. 50472022). The Advanced Light Source is supported by the Director, Office of Science, Office of Basic Energy Sciences, of the U.S. Department of Energy under Contract No. DE-AC02-05CH11231.

■ REFERENCES

(1) For recent reviews, see (a) *Endofullerenes: A New Family of Carbon Clusters*; Akasaka, T., Nagase, S., Eds.; Kluwer: Dordrecht, The Netherlands, 2002. (b) *Chemistry of Nanocarbons*; Akasaka, T., Wudl, F., Nagase, S., Eds.; John Wiley & Sons: Chichester, 2010. (c) Lu, X.; Akasaka, T.; Nagase, S.; Rare Earth Metals Trapped inside Fullerenes—Endohedral Metallofullerenes. In *Rare Earth Coordination Chemistry: Fundamentals and Applications*; Huang, C. H., Ed.; John Wiley & Sons: Singapore, 2010; pp 273−308. (d) Chaur, M. N.; Melin, F.; Ortiz, A. L.; Echegoyen, L. *Angew. Chem., Int. Ed.* **2009**, *48*, 7514. (e) Dunsch, L.; Yang, S. *Small* **2007**, *3*, 1298. (f) Yamada, M.; Akasaka, T.; Nagase, S. *Acc. Chem. Res.* **2010**, *43*, 92–102. (g) Osuna, S.; Swart, M.; Sola, M. *Phys. Chem. Chem. Phys.* **2011**, *13*, 3585. (h) Lu, X.; Akasaka, T.; Nagase, S. *Chem. Commun.* **2011**, *47*, 5942. (i) Liu, G.; Wu, Y.; Porfyrakis, K. *Curr. Org. Chem.* **2011**, *15*, 1197. (j) Rodríguez-Fortea, A.; Balch, A. L.; Poblet, J. M. *Chem. Soc. Rev.* **2011**, *40*, 3551.

(2) Takata, M.; Umeda, B.; Nishibori, E.; Sakata, M.; Saito, Y.; Ohno, M.; Shinohara, H. *Nature* **1995**, *377*, 46.

(3) (a) Iiduka, Y.; Wakahara, T.; Nakahodo, T.; Tsuchiya, T.; Sakuraba, A.; Maeda, Y.; Akasaka, T.; Yoza, K.; Horn, E.; Kato, T.; Liu, M. T. H.; Mizorogi, N.; Kobayashi, K.; Nagase, S. *J. Am. Chem. Soc.* **2005**, *127*, 12500. (b) Akasaka, T.; et al. *J. Am. Chem. Soc.* **2008**, *130*, 12840. (c) Lu, X.; Nikawa, H.; Feng, L.; Tsuchiya, T.; Maeda, Y.; Akasaka, T.; Mizorogi, N.; Slanina, Z.; Nagase, S. *J. Am. Chem. Soc.* **2009**, *131*, 12066.

(4) (a) Lu, X.; Slanina, Z.; Akasaka, T.; Tsuchiya, T.; Mizorogi, N.; Nagase, S. *J. Am. Chem. Soc.* **2010**, *132*, 5896. (b) Akasaka, T. et al. *J. Am. Chem. Soc.* **2000**, *122*, 9316.

(5) (a) Lee, H. M.; Olmstead, M. M.; Iezzi, E.; Duchamp, J. C.; Dorn, H. C.; Balch, A. L. *J. Am. Chem. Soc.* **2002**, *124*, 3494. (b) Maeda, Y.; et al. *J. Am. Chem. Soc.* **2004**, *126*, 6858. (c) Shustova, N. B.; Chen, Y. S.; Mackey, M. A.; Coumbe, C. E.; Phillips, J. P.; Stevenson, S.; Popov, A. A.; Boltalina, O. V.; Strauss, S. H. *J. Am. Chem. Soc.* **2009**, *131*, 17630. (d) Akasaka, T.; Lu, X.; Kuga, H.; Nikawa, H.; Mizorogi, N.; Slanina, Z.; Tsuchiya, T.; Yoza, K.; Nagase, S. *Angew. Chem., Int. Ed.* **2010**, *49*, 9715. (e) Lu, X.; Nikawa, H.; Tsuchiya, T.; Akasaka, T.; Toki, M.; Sawa, H.; Mizorogi, N.; Nagase, S. *Angew. Chem., Int. Ed.* **2010**, *49*, 594.

(6) (a) Olmstead, M. M.; de Bettencourt-Dias, A.; Duchamp, J. C.; Stevenson, S.; Dorn, H. C.; Balch, A. L. *J. Am. Chem. Soc.* **2000**, *122*, 12220. (b) Olmstead, M. H.; de Bettencourt-Dias, A.; Duchamp, J. C.; Stevenson, S.; Marciu, D.; Dorn, H. C.; Balch, A. L. *Angew. Chem., Int. Ed.* **2001**, *40*, 1223. (c) Olmstead, M. M.; Lee, H. M.; Duchamp, J. C.; Stevenson, S.; Marciu, D.; Dorn, H. C.; Balch, A. L. *Angew. Chem., Int. Ed.* **2003**, *42*, 900. (d) Beavers, C. M.; Zuo, T. M.; Duchamp, J. C.; Harich, K.; Dorn, H. C.; Olmstead, M. M.; Balch, A. L. *J. Am. Chem. Soc.* **2006**, *128*, 11352.(e) Zuo, T. M.; Beavers, C. M.; Duchamp, J. C.; Campbell, A.; Dorn, H. C.; Olmstead, M. M.; Balch, A. L. *J. Am. Chem. Soc.* **2007**, *129*, 2035.(f) Beavers, C. M.; Chaur, M. N.; Olmstead, M. M.; Echegoyen, L.; Balch, A. L. *J. Am. Chem. Soc.* **2009**, *131*, 11519. (g) Mercado, B. Q.; Chen, N.; Rodriguez-Fortea, A.; Mackey, M. A.; Stevenson, S.; Echegoyen, L.; Poblet, J. M.; Olmstead, M. M.; Balch, A. L. *J. Am. Chem. Soc.* **2011**, *133*, 6752.

(7) Stevenson, S.; Rice, G.; Glass, T.; Harich, K.; Cromer, F.; Jordan, M. R.; Craft, J.; Hadju, E.; Bible, R.; Olmstead, M. M.; Maitra, K.; Fisher, A. J.; Balch, A. L.; Dorn, H. C. *Nature* **1999**, *401*, 55.

(8) (a) Olmstead, M. M.; de Bettencourt-Dias, A.; Stevenson, S.; Dorn, H. C.; Balch, A. L. *J. Am. Chem. Soc.* **2002**, *124*, 4172. (b) Olmstead, M. M.; Lee, H. M.; Stevenson, S.; Dorn, H. C.; Balch, A. L. *Chem. Commun.* **2002**, 2688.

(9) Reich, A.; Panthofer, M.; Modrow, H.; Wedig, U.; Jansen, M. *J. Am. Chem. Soc.* **2004**, *126*, 14428.

(10) Che, Y. L.; Yang, H.; Wang, Z. M.; Jin, H. X.; Liu, Z. Y.; Lu, C. X.; Zuo, T. M.; Dorn, H. C.; Beavers, C. M.; Olmstead, M. M.; Balch, A. L. *Inorg. Chem.* **2009**, *48*, 6004.

(11) Yang, H.; Jin, H. X.; Zhen H. Wang, Z. M.; Liu, Z. Y.; Beavers, Mercado, B. Q.; C., M.; Olmstead, M. M.; Balch, A. L. *J. Am. Chem. Soc.* **2011**, *133*, 6299.

(12) Xu, J. X.; Lu, X.; Zhou, X. H.; He, X. R.; Shi, Z. J.; Gu, Z. N. *Chem. Mater.* **2004**, *16*, 2959.

(13) Nikawa, H.; Yamada, T.; Cao, B. P.; Mizorogi, N.; Slanina, Z.; Tsuchiya, T.; Akasaka, T.; Yoza, K.; Nagase, S. *J. Am. Chem. Soc.* **2009**, *131*, 10950.

(14) Kurihara, H.; Lu, X.; Iiduka, Y.; Mizorogi, N.; Slanina, Z.; Tsuchiya, T.; Akasaka, T.; Nagase, S. *J. Am. Chem. Soc.* **2011**, *133*, 2382.

(15) (a) Yang, H.; Beavers, C. M.; Wang, Z. M.; Jiang, A.; Liu, Z. Y.; Jin, H. X.; Mercado, B. Q.; Olmstead, M. M.; Balch, A. L. *Angew. Chem., Int. Ed.* **2010**, *49*, 886. (b) Yang, H.; Mercado, B. Q.; Jin, H. X.; Wang, Z. M.; Jiang, A.; Liu, Z. Y.; Beavers, C. M.; Olmstead, M. M.; Balch, A. L. *Chem. Commun.* **2011**, *47*, 2068.

(16) (a) Sheng, E.; Wang, S.; Yang, G; Zhou, S; Cheng, L.; Zhang, K.; Huang, Z. *Organometallics* **2003**, *22*, 684. (b) Deacon, G. B.; Forsyth, C. M. *Organometallics* **2003**, *22*, 1349.

(17) (a) Kobayashi, K.; Nagase, S. *Chem. Phys. Lett.* **1998**, *282*, 325. (b) Mizorogi, N.; Nagase, S. *Chem. Phys. Lett.* **2006**, *431*, 110.

(18) Frisch, M. J. et al. GAUSSIAN 03, Revision C. 01; Gaussian Inc.: Wallingford, CT, 2004.

(19) Binkley, J. S.; Pople, J. A.; Hehre, W. J. *J. Am. Chem. Soc.* **1980**, *102*, 939.

(20) Cundari, T. R.; Stevens, W. J. *J. Chem. Phys.* **1993**, *98*, 5555.

(21) Hariharan, P. C.; Pople, J. A. *Theor. Chim. Acta* **1973**, *28*, 213.

(22) Cao, X. Y.; Dolg, M. *J. Mol. Struct. (Theochem)* **2002**, *581*, 139.

(23) (a) Becke, A. D. *Phys. Rev. A* **1988**, *38*, 3098. (b) Becke, A. D. *J. Chem. Phys.* **1993**, *98*, 5648. (c) Lee, C.; Yang, W.; Parr, R. G. *Phys. Rev. B* **1988**, *37*, 785.